Regular Article

blood

LYMPHOID NEOPLASIA

Sensitivity to PI3K and AKT inhibitors is mediated by divergent molecular mechanisms in subtypes of DLBCL

Tabea Erdmann,[1-3] Pavel Klener,[4,5] James T. Lynch,[6] Michael Grau,[1,2] Petra Vočková,[4,5] Jan Molinsky,[4,5] Diana Tuskova,[4,5] Kevin Hudson,[6] Urszula M. Polanska,[6] Michael Grondine,[7] Michele Mayo,[7] Beiying Dai,[1,2] Matthias Pfeifer,[8] Kristian Erdmann,[1,2] Daniela Schwammbach,[1,2] Myroslav Zapukhlyak,[1,2] Annette M. Staiger,[9,10] German Ott,[9] Wolfgang E. Berdel,[2,11] Barry R. Davies,[6] Francisco Cruzalegui,[6] Marek Trneny,[4,5] Peter Lenz,[12] Simon T. Barry,[6] and Georg Lenz[1,2,11]

[1]Translational Oncology, University Hospital Münster, Münster, Germany; [2]Cluster of Excellence EXC 1003, Cells in Motion, Münster, Germany; [3]Fachbereich Chemie und Pharmazie, University of Münster, Münster, Germany; [4]Institute of Pathological Physiology, First Faculty of Medicine, Charles University Prague, Prague, Czech Republic; [5]First Medical Department, Department of Hematology, Charles University General Hospital Prague, Prague, Czech Republic; [6]Innovative Medicines and Early Development (IMED) Oncology AstraZeneca, Li Ka Shing Centre, Cambridge, United Kingdom; [7]IMED Oncology AstraZeneca, Gatehouse Park, Boston, MA; [8]Division of Cancer, Department of Surgery & Cancer, Imperial College, London, United Kingdom; [9]Department of Clinical Pathology, Robert-Bosch-Hospital, Stuttgart, Germany; [10]Dr. Margarete Fischer-Bosch-Institute of Clinical Pharmacology, Stuttgart, Germany; [11]Department of Medicine A, Hematology, Oncology, and Pneumology, University Hospital Münster, Münster, Germany; and [12]Department of Physics, Philipps University, Marburg, Germany

Key Points

- PI3Kα/δ inhibition induces cytotoxicity in ABC DLBCLs through downregulation of NF-κB signaling.
- Inhibition of AKT induces cytotoxicity by downregulation of MYC in PTEN-deficient DLBCL models in vivo and in vitro.

Activated B-cell-like (ABC) and germinal center B-cell-like diffuse large B-cell lymphoma (DLBCL) represent the 2 major molecular DLBCL subtypes. They are characterized by differences in clinical course and by divergent addiction to oncogenic pathways. To determine activity of novel compounds in these 2 subtypes, we conducted an unbiased pharmacologic in vitro screen. The phosphatidylinositol-3-kinase (PI3K) α/δ (PI3Kα/δ) inhibitor AZD8835 showed marked potency in ABC DLBCL models, whereas the protein kinase B (AKT) inhibitor AZD5363 induced apoptosis in PTEN-deficient DLBCLs irrespective of their molecular subtype. These in vitro results were confirmed in various cell line xenograft and patient-derived xenograft mouse models in vivo. Treatment with AZD8835 induced inhibition of nuclear factor κB signaling, prompting us to combine AZD8835 with the Bruton's tyrosine kinase inhibitor ibrutinib. This combination was synergistic and effective both in vitro and in vivo. In contrast, the AKT inhibitor AZD5363 was effective in PTEN-deficient DLBCLs through downregulation of the oncogenic transcription factor MYC. Collectively, our data suggest that patients should be stratified according to their oncogenic dependencies when treated with PI3K and AKT inhibitors. (*Blood*. 2017;130(3):310-322)

Introduction

Diffuse large B-cell lymphoma (DLBCL) is the most common lymphoma subtype, representing roughly 30% to 40% of all cases.[1] DLBCL is a heterogeneous tumor entity,[2] but according to gene expression profiling (GEP), 2 major molecular subtypes termed activated B-cell-like (ABC) and germinal center B-cell-like (GCB) DLBCL can be distinguished.[3] ABC and GCB DLBCLs are addicted to different signaling pathways, rendering them sensitive or resistant to specific pathway inhibitors.[4] Especially as relapsed DLBCL patients experience adverse survival, novel therapeutic strategies are warranted.[5]

Previous work has shown activation of the oncogenic phosphatidylinositol-3-kinase (PI3K)/protein kinase B (AKT) pathway in a significant number of primary DLBCL samples using immunohistochemistry.[6,7] This dependency is detectable in different molecular DLBCL subtypes.[8-10] Activated PI3K isoforms phosphorylate phosphatidylinositol-4,-5-bisphosphate to phosphatidyl-inositol-3,-4,-5-trisphosphate (PIP^3), which activates AKT, whereas the tumor suppressor PTEN as major negative regulator of PI3K/AKT dephosphorylates PIP^3.[11,12] In GCB DLBCLs, PTEN loss seems to be the predominant mechanism of PI3K/AKT activation, whereas in other DLBCL subtypes, activation is associated with constitutive B-cell receptor signaling.[8-10] Prior studies suggested that PI3K inhibition alone or in combination with other compounds might be a promising therapeutic strategy for DLBCL patients. However, in these analyses, rather unspecific compounds were used.[9,13,14] The clinical usefulness of PI3K inhibition was called into question based on a small clinical study investigating the efficacy of the PI3K δ (PI3Kδ) inhibitor idelalisib as

Submitted 20 December 2016; accepted 10 February 2017. Prepublished online as *Blood* First Edition paper, 15 February 2017; DOI 10.1182/blood-2016-12-758599.

The data reported in this article have been deposited in the Gene Expression Omnibus database (accession number GSE92619).

The online version of this article contains a data supplement.

There is an Inside *Blood* Commentary on this article in this issue.

The publication costs of this article were defrayed in part by page charge payment. Therefore, and solely to indicate this fact, this article is hereby marked "advertisement" in accordance with 18 USC section 1734.

none of the treated DLBCL patients responded.[15] Using a pharmacologic screen, we were able to unravel, in this study, that different molecular subtypes are highly sensitive to specific PI3K/AKT inhibitors, indicating that this pathway represents a promising target for DLBCL patients.

Materials and methods

Cell culture, retroviral constructs, and transductions

The experiments were performed as described.[16-18] Protocols are available in the supplemental Materials and methods, available on the *Blood* Web site. Sequences of short hairpin RNAs (shRNAs) are summarized in supplemental Table 1.

Pharmacologic screen

Protocols are available in the supplemental Materials and methods. Sensitivity of a cell line to inhibitor treatment was defined as a 50% inhibitory concentration (IC_{50}) < 1 μM.

In vitro viability assay and inhibitor studies

Cell viability following compound treatment was determined after 5 days using the Cell Titer Glo assay (Promega, Madison, WI) as previously described.[19,20] Previous studies investigating the selectivity profile of AZD8835 and AZD5363 have indicated that AZD8835 is a selective PI3K α/δ (PI3Kα/δ) and AZD5363 is a selective AKT inhibitor.[21-23]

In vivo xenograft mouse studies

Protocols are available in the supplemental Materials and methods.

GEP

GEP was performed after AZD8835[23] or AZD5363[22] treatment as previously described.[18] Protocols are available in the supplemental Materials and methods.

Quantitative PCR

Quantitative PCR was performed as described using predesigned assays (Applied Biosystems, Carlsbad, CA).[17]

Western blotting

Western blotting was performed as described previously.[24] The antibodies used are summarized in supplemental Table 2.

Carboxyfluorescein succinimidyl ester (CFSE) proliferation and Annexin-V staining

Protocols are available in the supplemental Materials and methods.

Nuclear fractionation

Cells were treated for 6 and 24 hours with AZD8835 or dimethyl sulfoxide (DMSO). Cytosolic and nuclear fractions were prepared using the Subcellular Protein Fractionation Kit for Cultured Cells (Thermo Fisher Scientific, Waltham, MA).

Results

A pharmacologic screen identifies divergent sensitivity to PI3K/AKT inhibitors in molecular DLBCL subtypes

To identify novel targets for the treatment of DLBCL, we performed a pharmacologic screen utilizing compounds inhibiting pathways involved in proliferation, survival, and apoptosis (Figure 1A). To also identify compounds that are effective only in specific DLBCL subtypes, we screened 4 GCB (K422, HT, BJAB, and OCI-Ly2) and 4 ABC DLBCL (OCI-Ly3, U2932, TMD8, and HBL-1) models and determined viability after inhibitor treatment. As positive controls, we used the chemotherapeutic agent doxorubicin that was toxic to all 8 cell lines and the Bruton's tyrosine kinase (BTK) inhibitor ibrutinib that induced cytotoxicity in ABC DLBCLs without *CARD11* mutations, as previously described.[25] The vast majority of compounds had only little or no effect on the cell lines, suggesting that the affected pathways might not be crucial for survival. In contrast, ABC DLBCL models were highly sensitive to the PI3Kα/δ inhibitor AZD8835, whereas viability of GCB DLBCL lines was significantly reduced following AKT inhibition using AZD5363 (Figure 1A).[22,23] In contrast, only TMD8 cells were highly sensitive ($IC_{50} = 0.25$ μM), and HT cells ($IC_{50} = 0.86$ μM) were moderately sensitive to the PI3Kδ inhibitor idelalisib.

PI3K and AKT inhibitors are effective in DLBCL subgroups

To determine if AZD8835 and AZD5363 indeed represent promising compounds for the treatment of molecular DLBCL subtypes, we expanded our analyses to 15 DLBCL models. Molecular characteristics for these 15 cell lines are summarized in Table 1. First, we determined the expression status of the PI3Kα and PI3Kδ isoforms, the phosphorylation status of AKT as marker of pathway activation, as well as expression of PTEN. PI3Kα and PI3Kδ expression was found virtually in all models, although expression levels varied (Figure 1B; supplemental Figure 1A). Activation of AKT was detectable in most of the cell lines, whereas PTEN was lost in the majority of GCB DLBCLs (Figure 1C; supplemental Figure 1B).

Next, we treated these lines with AZD8835 and AZD5363. Four of 5 ABC DLBCL, but only 1 GCB DLBCL line, were sensitive to AZD8835 ($P = .017$; Figure 1D). In contrast, AZD5363 reduced viability in 1 ABC DLBCL model, but in 8 of 10 GCB DLBCLs ($P = .047$; Figure 1D). As mainly GCB DLBCLs were sensitive to AZD5363, sensitivity to AKT inhibition was correlated to the PTEN expression status. Seven of the 9 sensitive lines were PTEN-deficient, whereas all of the insensitive lines expressed PTEN, suggesting that predominantly PTEN-deficient DLBCLs respond to AKT inhibition ($P = .0056$; Figure 1E). Interestingly, 1 of the PTEN-deficient models was the ABC DLBCL line U2932, suggesting that the PTEN expression status overrides the molecular subtype with respect to AKT inhibitor sensitivity. In summary, these results indicate that different molecular DLBCL subtypes are addicted to different branches of the PI3K/AKT pathway.

AKT inhibition induces apoptosis and reduces cell proliferation

To gain insights into the mechanisms underlying the AZD5363-induced toxicity, cell proliferation and the rate of apoptosis were measured in 2 sensitive (K422 and BJAB) and 1 resistant (HBL-1) DLBCL model. AZD5363 induced apoptosis measured by Annexin-V/propidium iodide (PI) staining in BJAB but not in K422 or HBL-1 cells (Figure 2A). In contrast, proliferation determined by CFSE staining was markedly reduced in sensitive K422 and BJAB cells, whereas resistant HBL-1 cells were unaffected (Figure 2B).

AZD5363 is active in vivo

We next determined if AZD5363 sensitivity of PTEN-deficient DLBCLs translates into an in vivo setting. To this end, we created xenograft mouse models of the 2 PTEN-deficient GCB DLBCL lines K422 and

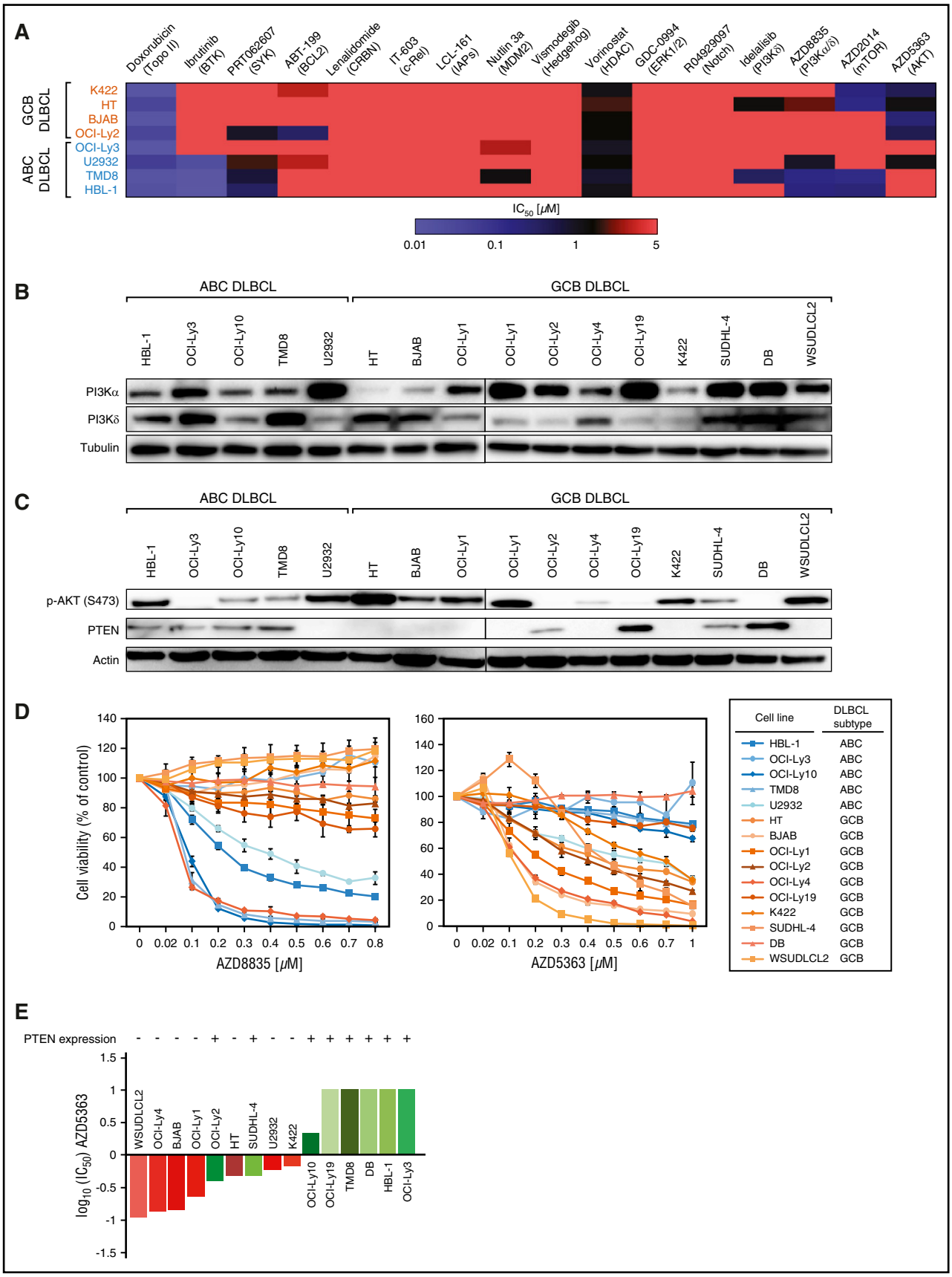

Figure 1. PI3Kα/δ and AKT inhibitors are active in molecular DLBCL subtypes. (A) Heat map of IC_{50} concentrations for 16 inhibitors across 8 DLBCL cell lines. Red indicates resistance, whereas blue indicates sensitivity ($IC_{50} < 1$ μM) to a specific compound. Doxorubicin and ibrutinib are used as positive control inhibitors. (B) Western blot analysis of PI3Kα and PI3Kδ isoform expression. Lysates from OCI-Ly1 cells are used on both blots to allow a comparison of basal protein expression. Representative results

Table 1. Molecular characteristics of DLBCL cell lines

Cell line	DLBCL subtype	PTEN expression	Chronic active B-cell receptor signaling	Ibrutinib sensitivity	AZD8835 sensitivity	AZD5363 sensitivity	*MYC* aberrations
HBL-1	ABC	Yes	Yes[25]	Yes*	Yes	No	Rearrangement[41]
OCI-Ly3	ABC	Yes	No[25]	No*	No	No	Amplification[41]
OCI-Ly10	ABC	Yes	Yes[25]	Yes[25]	Yes	No	Amplification[20]
TMD8	ABC	Yes	Yes[25]	Yes*	Yes	No	n.a.
U2932	ABC	No	Yes[25]	Yes*	Yes	Yes	n.a.
HT	GCB	No	n.a.	No*	No	Yes	n.a.
BJAB	GCB	No	No[25]	No*	No	Yes	Amplification[20]
OCI-Ly1	GCB	No	n.a.	No†	No	Yes	Amplification[42]
OCI-Ly2	GCB	Yes	n.a.	No*	No	Yes	wt[42]
OCI-Ly4	GCB	No	n.a.	No†	Yes	Yes	Rearrangement[42]
OCI-Ly19	GCB	Yes	No[25]	No[25]	No	No	Rearrangement[43]
K422	GCB	No	n.a.	No*	No	Yes	Rearrangement[44]
SUDHL-4	GCB	Yes	n.a.	No†	No	Yes	Amplification[41]
DB	GCB	Yes	n.a.	n.a.	No	No	Amplification[9]
WSUDLCL2	GCB	No	n.a.	n.a.	No	Yes	Amplification[45]

n.a., not available; wt, wild type.
*Data shown in Figure 1A.
†Data not shown.

WSUDLCL2. Treatment of both models with AZD5363 resulted in significantly reduced tumor growth compared with vehicle-treated mice ($P = .029$ for AZD5363 vs vehicle on day 18 in K422; $P = .036$ for AZD5363 vs vehicle on day 11 in WSUDLCL2; Figure 2C).

To analyze if AZD5363 activity translates into a setting of relapsed/refractory DLBCL patients, we used a cell line (UPF4D) and a corresponding patient-derived xenograft (PDX) mouse model (WEHA) from a refractory GCB DLBCL patient.[26] UPF4D cells showed high levels of phospho-AKT (p-AKT) and complete absence of PTEN (Figure 2D). Subsequent in vitro treatment of these cells showed complete resistance to AZD8835 but high sensitivity to AZD5363 with strong induction of apoptosis (Figure 2E-F), further suggesting that AKT activation promotes tumor growth in PTEN-deficient DLBCLs. Application of AZD5363 to the corresponding PDX mouse model WEHA resulted in significantly decreased tumor growth compared with vehicle-treated mice ($P = 7.86 \times 10^{-7}$ for AZD5363 vs vehicle on day 11; Figure 2G). The effect was even stronger than in the cell line xenograft models, indicating that AZD5363 activity translates into a relapsed/refractory DLBCL patient setting.

AKT inhibition downregulates MYC signaling in DLBCLs

Next, we investigated the molecular mechanisms of AZD5363 activity in different DLBCL models. As an ATP-competitive inhibitor that promotes AKT membrane localization and subsequent AKT phosphorylation, AZD5363 treatment of 6 and 24 hours strongly increased p-AKT levels in the PTEN-deficient lines BJAB, K422, and U2932 (Figure 3A).[22,27] Phosphorylation of the AKT target PRAS40, an mTOR inhibitor in its unphosphorylated state, was completely lost, indicating inhibition of mTOR by AZD5363. These results were confirmed in UPF4D cells (Figure 3B).

To elucidate which biologic processes are affected by AZD5363 treatment, GEP was performed after 6, 12, 18, and 24 hours of AZD5363 incubation in 2 PTEN-deficient and AZD5363-sensitive cell lines (K422 and U2932). A common gene expression signature was created consisting of genes that were consistently down- or upregulated across all time points in both lines (Figure 3C; supplemental Figure 2; supplemental Table 3). This analysis revealed 96 genes that were significantly downregulated ($P \leq 2.5 \times 10^{-4}$; false discovery rate [FDR] = .006) and 97 genes that were significantly upregulated ($P \leq 2.5 \times 10^{-4}$; FDR = .012). To analyze in an unbiased fashion which biological processes are affected by AZD5363, we performed a gene set enrichment analysis using a database of 16.963 gene expression signatures.[28-32] This approach revealed that 14 previously described MYC target gene signatures were significantly enriched with down-regulated genes following AZD5363 treatment, suggesting that AKT inhibition downregulates the transcription factor MYC (Figure 3D; supplemental Tables 4 and 5). In addition, previously described gene sets correlated with metabolism were enriched with downregulated genes (supplemental Table 4). In contrast, only 1 of 11 previously described PI3K/AKT gene signatures was significantly enriched with downregulated genes and only at moderate levels (supplemental Table 6). This signature was created in the PTEN-deficient GCB DLBCL cell line HT following PTEN reexpression, suggesting that PTEN target genes at least partially overlap with genes controlled by AKT signaling.[9]

To verify the GEP results, we determined MYC expression following AZD5363 treatment on messenger RNA (mRNA) and protein levels. *MYC* mRNA expression was not downregulated by AZD5363 ($\log_2$(ratio) = .0682) as shown by our GEP data. In contrast, MYC protein levels were significantly reduced after 6 and 24 hours of AZD5363 treatment in sensitive BJAB, K422, and U2932 cells (Figure 3E). To determine to what extent MYC downregulation

Figure 1 (continued) from at least 3 independent experiments are shown. (C) Western blot analysis of AKT phosphorylation and PTEN expression. Lysates from OCI-Ly1 cells are used on both blots to allow a comparison of basal protein expression. Representative results from at least 2 independent experiments are shown. (D) AZD8835 is predominantly effective in ABC DLBCL models, whereas AZD5363 induces cytotoxicity mostly in GCB DLBCL cell lines. Representative results from at least 3 independent experiments are shown. Error bars indicate standard deviations. (E) AZD5363 predominantly affects PTEN-deficient DLBCLs. Depiction of $\log_{10}$-normalized IC_{50} values demonstrates that PTEN-negative (red) DLBCL models are significantly more sensitive to AKT inhibition compared with PTEN-expressing (green) cell lines ($P = .0056$; 1-tailed Fisher's exact test).

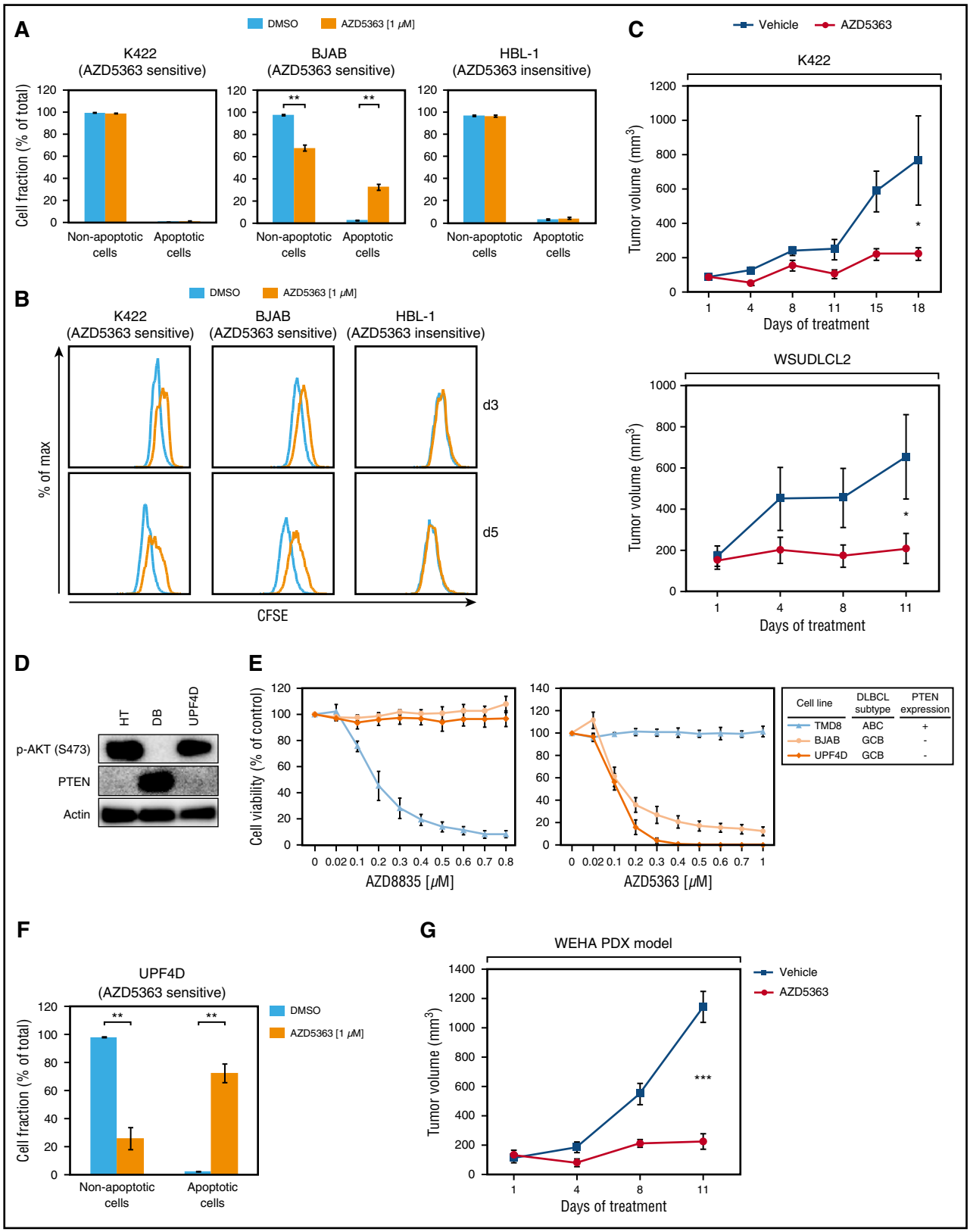

Figure 2. AZD5363 is highly active in vitro and in vivo. (A) AZD5363 treatment induces apoptosis. Five days of inhibitor treatment results in a significant increase of apoptosis in BJAB, whereas no induction of apoptosis is detectable in K422 and HBL-1 cells. Data are expressed as means ± standard deviation of at least 3 independent experiments. (B) AKT inhibitor treatment reduces cell proliferation. CFSE dilutions are measured 3 and 5 days after treatment with AZD5363. In K422 and BJAB cells, proliferation is markedly decreased by AZD5363. Representative results of 3 independent experiments are shown. (C) Tumor growth curves for K422 and WSUDLCL2 xenograft mouse models. AZD5363 treatment (red) significantly reduces tumor growth compared with the vehicle control (blue) in both xenograft mouse models ($P = .029$ for AZD5363 [n = 9] vs vehicle [n = 8] on day 18 in K422; $P = .036$ for AZD5363 [n = 9] vs vehicle [n = 9] on day 11 in WSUDLCL2; 1-tailed 2-sample Student *t* tests). Treatment was initiated after animals developed macroscopic signs of tumors (day 19 after engraftment in K422; day 32 after engraftment in WSUDLCL2). Error bars indicate the

contributes to the AZD5363-induced cytotoxicity, we performed an MYC rescue experiment. By transducing either an *MYC* complementary DNA (cDNA) or an empty vector into the AZD5363-sensitive models BJAB and U2932, we could detect a substantial MYC-induced rescue after AZD5363 treatment, indicating that the observed MYC downregulation contributes at least partially to its toxic effects (Figure 3F). To investigate whether this rescue effect is specific to AZD5363, we determined viability of these MYC-expressing cells after doxorubicin treatment. No resistance against doxorubicin was conferred by *MYC* cDNA expression, indicating the specificity of our findings (Figure 3F).

In summary, our in vitro and in vivo data indicate that AKT inhibition might represent a promising therapeutic approach in PTEN-deficient DLBCLs independent of their molecular subtype. The cytotoxic phenotype seems to be at least partially caused by downregulation of MYC.

Simultaneous inhibition of PI3Kα and PI3Kδ is necessary to induce cytotoxicity in ABC DLBCLs

Our pharmacologic screen identified the PI3Kα/δ inhibitor AZD8835 to be highly active predominantly in ABC DLBCLs (Figure 1A,D). In contrast, the PI3Kδ-specific inhibitor idelalisib was highly effective only in 1 DLBCL model, consistent with limited efficacy in DLBCLs in a small clinical trial.[15] This finding led us to investigate if inhibition of both PI3Kα and PI3Kδ is required to induce cytotoxicity in ABC DLBCLs. To this end, PI3Kα was knocked down using a specific shRNA and cells were treated subsequently with either idelalisib or DMSO. Knockdown of PI3Kα in combination with DMSO was not toxic to HBL-1 and OCI-Ly10 cells, whereas addition of idelalisib showed strong cytotoxicity in both lines (Figure 4A). AZD8835-insensitive BJAB cells as a negative control were unaffected by PI3Kα knockdown and idelalisib treatment, confirming the AZD8835 viability assay (Figures 1D and 4A). To validate the specificity of our approach, HBL-1, OCI-Ly10, and BJAB cells carrying either a nontoxic *MSMO1* shRNA or a toxic *MYC* shRNA were treated with either DMSO or idelalisib. As expected, these cells were completely unaffected by idelalisib (supplemental Figure 3). In summary, our results implicate that simultaneous inhibition of both PI3Kα and PI3Kδ is required to induce cytotoxicity in ABC DLBCLs.

AZD8835 results in apoptosis induction and inhibition of proliferation

To identify the mechanisms responsible for AZD8835-mediated cytotoxicity, induction of apoptosis was analyzed using Annexin-V/PI staining in 2 sensitive (HBL-1 and TMD8) and 1 insensitive (BJAB) model. Predominantly in HBL-1 and less pronounced in TMD8 cells, a significant increase in apoptotic cells was observed, whereas no apoptosis was detectable in BJAB cells (Figure 4B). Analyses of proliferation after AZD8835 treatment using CFSE staining showed strongly decreased proliferation in HBL-1 and TMD8 but not in BJAB cells (Figure 4C). These results suggest that PI3Kα/δ inhibition results in induction of apoptosis and inhibition of proliferation in ABC DLBCLs.

PI3Kα/δ inhibition is effective in ABC DLBCL models in vivo

To analyze in vivo activity of AZD8835, we created xenograft mouse models of the 2 ABC DLBCL cell lines OCI-Ly10 and TMD8. AZD8835 can be administered using 2 schedules, 25 mg/kg twice a day continuously and 100 mg/kg twice a day on day 1/day 4 that have been shown to be equally effective.[23] Both schedules significantly reduced tumor growth in our models ($P = .0091$ for AZD8835 vs vehicle on day 22 in TMD8 [25 mg/kg twice a day continuously]; $P = .0003$ for AZD8835 vs vehicle on day 11 in OCI-Ly10 [100 mg/kg twice a day on day 1/day 4]; Figure 4D). To verify these in vivo data in a setting of relapsed/refractory DLBCL patients, we used the PDX model KTC, which was derived from a treatment-refractory non-GCB DLBCL patient.[26] AZD8835 significantly decreased tumor growth in the KTC model ($P = 5.36 \times 10^{-5}$ for AZD8835 vs vehicle on day 15 [100 mg/kg twice a day on day 1/day 4]; Figure 4E), suggesting that PI3Kα/δ inhibition is effective in ABC DLBCLs in vivo.

AZD8835 inhibits NF-κB signaling in ABC DLBCLs

To investigate molecular effects of PI3Kα/δ inhibition in ABC DLBCLs, we analyzed sensitive U2932 and HBL-1 cells after 6 and 24 hours of AZD8835 treatment. Inhibition of PI3Kα/δ induced a strong p-AKT decrease at both time points. PRAS40 phosphorylation was decreased as well, but to a lesser degree compared with AZD5363-treated cells (Figures 3A and 5A).

To investigate which signaling cascades are affected by AZD8835 treatment in ABC DLBCLs, GEP was performed after 6, 12, 18, and 24 hours of PI3Kα/δ inhibition in sensitive U2932, HBL-1, and OCI-Ly10 cells. A common gene expression signature from these lines was created revealing 96 genes that were significantly downregulated ($P \leq 2.5 \times 10^{-4}$; FDR = .009) and 94 genes significantly upregulated ($P \leq 2.5 \times 10^{-4}$; FDR = .009) after AZD8835 treatment (Figure 5B; supplemental Figure 4; supplemental Table 7). Interestingly, several known NF-κB target genes like *JUNB*, *NFKBIA*, *NFKBIE*, and *TNF* were detected among the top downregulated genes (Figure 5B), suggesting that PI3Kα/δ inhibition downregulates NF-κB signaling. To verify NF-κB inhibition after AZD8835 treatment, we performed an unbiased gene set enrichment analysis[32] using our signatures database.[28-31] Indeed, 12 previously described NF-κB target gene signatures were detected among the top downregulated gene sets, suggesting a crosstalk between the PI3K/AKT and the NF-κB pathway in ABC DLBCLs (Figure 5C; supplemental Tables 8 and 9). Interestingly, only 1 of the previously described PI3K/AKT gene expression signatures was moderately enriched with downregulated genes (supplemental Table 10). We also detected several MYC gene expression signatures to be significantly enriched with downregulated genes, indicating that PI3Kα/δ inhibition downregulates MYC signaling (supplemental Table 11). MYC protein downregulation following AZD8835 treatment was confirmed in 2 sensitive ABC DLBCL lines

Figure 2 (continued) standard error of the mean. (D) Western blotting for p-AKT and PTEN expression in the patient-derived GCB DLBCL cell line UPF4D. Lysates from HT and DB cells are used as a positive control for p-AKT and PTEN expression, respectively. (E) AZD8835 and AZD5363 viability assay in UPF4D cells in vitro. PI3Kα/δ inhibition does not affect viability of UPF4D cells compared with the positive control cell line TMD8. In contrast, AKT inhibition induces even stronger cytotoxicity in UPF4D cells compared with the positive control line BJAB. Data are expressed as means ± standard deviation of at least 3 independent experiments. (F) AZD5363 induces apoptosis in UPF4D cells after 24 hours measured by Annexin-V/PI staining. Data are expressed as means ± standard deviation of at least 3 independent experiments. (G) Tumor growth curves of the PDX mouse model WEHA. AZD5363 treatment (red) significantly decreases tumor growth compared with vehicle only treated mice (blue) ($P = 7.86 \times 10^{-7}$ for AZD5363 [n = 9] vs vehicle [n = 9] on day 11; 1-tailed 2-sample Student *t* test). Treatment was initiated after animals developed macroscopic signs of tumors (day 13 after engraftment). Error bars indicate the standard error of the mean. *$P < .05$; **$P < .01$; ***$P < .001$.

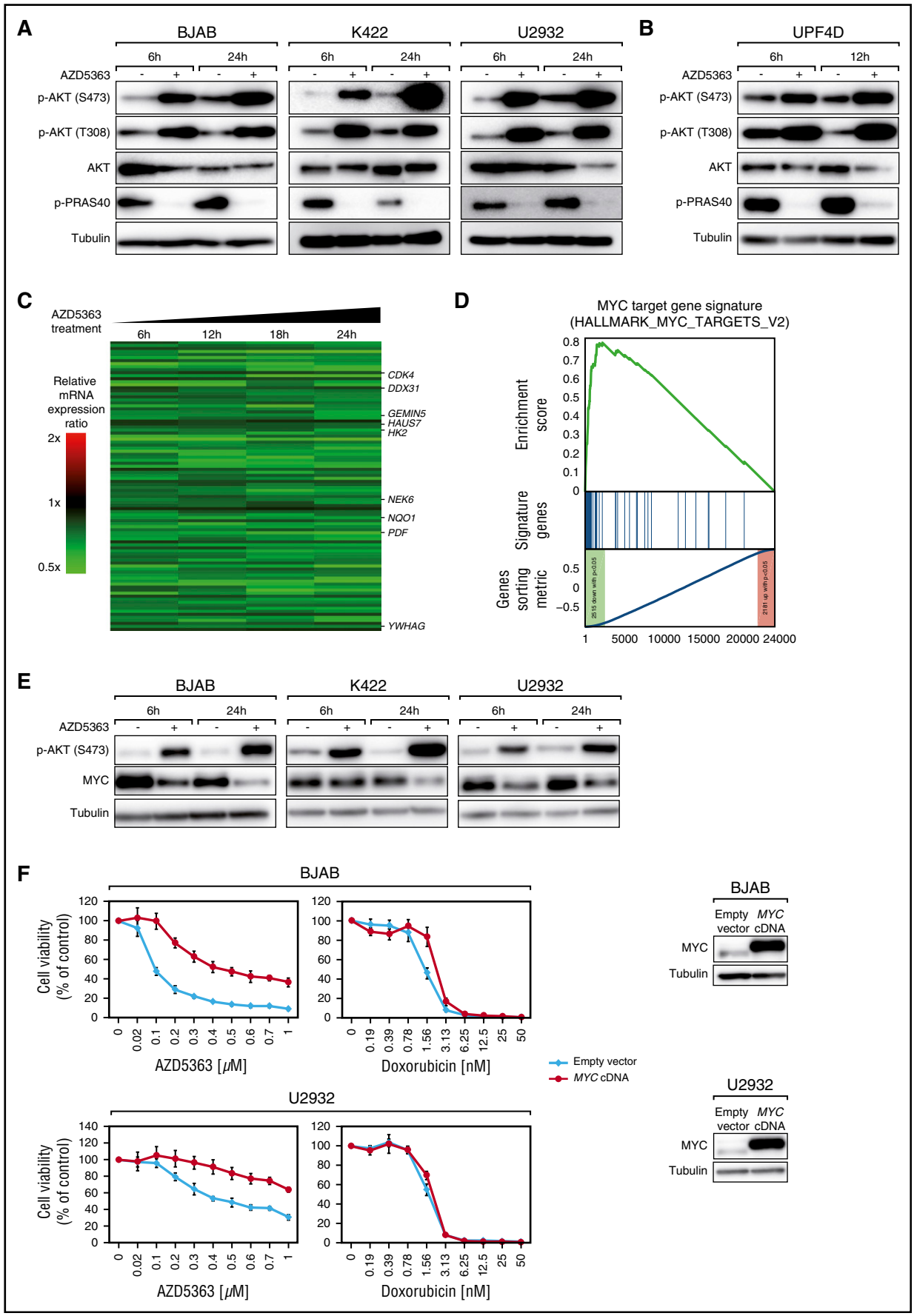

Figure 3.

(U2932 and HBL-1; supplemental Figure 5A), whereas MYC knockdown was not detectable in resistant GCB DLBCL models potentially explaining their insensitivity to PI3Kα/δ inhibition (supplemental Figure 5B).

In order to confirm the GEP data with respect to NF-κB signaling, NF-κB target gene expression levels were determined by quantitative PCR. For all target genes, a significant downregulation after 24 hours of AZD8835 treatment was detectable in sensitive HBL-1, OCI-Ly10, and TMD8 but not in resistant OCI-Ly3 and BJAB cells. The level of depletion was comparable to effects caused by the positive control inhibitor ibrutinib (Figure 5D). Western blotting in these 5 lines confirmed the knockdown for the NF-κB targets BCL-XL, IRF4, and IκB-ζ on protein levels in sensitive (HBL-1, OCI-Ly10, and TMD8) but not in insensitive models (OCI-Ly3 and BJAB), validating that PI3Kα/δ inhibition downregulates NF-κB signaling in AZD8835-sensitive ABC DLBCLs (Figure 5E).

Finally, to investigate NF-κB activity at the nuclear level, cytosolic and nuclear extracts from HBL-1, TMD8, U2932, OCI-Ly3, and BJAB cells were prepared following AZD8835 treatment of 6 and 24 hours. PI3Kα/δ inhibition significantly decreased nuclear expression levels of the NF-κB subunits RelA and p50 in sensitive (HBL-1, TMD8, and U2932) but not in insensitive models (OCI-Ly3 and BJAB), further confirming NF-κB pathway inhibition (Figure 5F).

Activating *CARD11* mutations cause resistance to PI3K inhibition

An interesting finding of our inhibitor screen was the insensitivity of the ABC DLBCL and NF-κB-dependent model OCI-Ly3 to PI3Kα/δ inhibition. Analyses of NF-κB target genes already indicated a lack of subsequent NF-κB inhibition in OCI-Ly3 (Figure 5D-E). This finding was further confirmed by analyzing p-IκB-α levels as marker of NF-κB activation. Whereas p-IκB-α levels markedly decreased in HBL-1 and TMD8 cells following AZD8835 treatment, no change was observable in OCI-Ly3 cells. In contrast, the IκB kinase inhibitor AFN700[33] significantly decreased p-IκB-α levels in all 3 models (Figure 5G), suggesting that AZD8835 resistance in OCI-Ly3 cells could be caused by lack of subsequent NF-κB inhibition.

OCI-Ly3 cells are characterized by the activating *CARD11*^{L244P} mutation leading to constitutive NF-κB signaling and ibrutinib resistance.[4,25,34] To assess if this mutation causes resistance to PI3Kα/δ inhibition, we transduced HBL-1 and TMD8 cells with either a *CARD11*^{L244P} cDNA or an empty vector (Figure 5H; supplemental Figure 6A). Subsequently, we treated these cells with AZD8835 or ibrutinib as a control inhibitor. Interestingly, expression of the *CARD11*^{L244P} mutation caused complete resistance to AZD8835 and ibrutinib in both models, suggesting that activating *CARD11* mutations can induce PI3Kα/δ inhibitor resistance (Figure 5H). Because we also detected an MYC downregulation after AZD8835 treatment (supplemental Table 11; supplemental Figure 5A), we assessed the contribution of MYC knockdown to the AZD8835-induced cytotoxicity. To this end, we transduced HBL-1 and TMD8 cells with either an *MYC* cDNA or an empty vector and treated these cells with AZD8835 (Figure 5I; supplemental Figure 6B). In HBL-1 cells, no rescue was observed, whereas only a moderate partial rescue was detectable in TMD8 cells (Figure 5I). These results imply that the cytotoxicity induced by PI3Kα/δ inhibition is predominantly caused by inhibition of NF-κB signaling rather than MYC downregulation.

Combined PI3Kα/δ and BTK inhibition is highly effective in ABC DLBCLs

Sensitivity to PI3Kα/δ inhibition seems to be predominantly caused by downregulation of NF-κB signaling. We treated 4 ABC DLBCL cell lines (OCI-Ly10, TMD8, HBL-1, and OCI-Ly3) with a combination of different AZD8835 and ibrutinib concentrations, to determine if simultaneous PI3Kα/δ and BTK inhibition might have synergistic effects on cell viability. Whereas the single agents had only modest effects, their combination resulted in synergistic effects in OCI-Ly10, TMD8, and HBL-1 cells. In contrast, OCI-Ly3 cells were not sensitive to either single drug or the combination (Figure 6A).

These observations were confirmed in vivo using xenograft mouse models of OCI-Ly10, TMD8, and the KTC PDX model. Single ibrutinib treatment only slightly affected tumor growth in all models consistent with previous reports.[35] In OCI-Ly10 and TMD8, AZD8835 alone resulted in growth reduction, while administration of both inhibitors almost completely abolished tumor growth ($P = .002$ for AZD8835 vs AZD8835/ibrutinib on day 11 in OCI-Ly10; $P = .001$ for AZD8835 vs AZD8835/ibrutinib on day 22 in TMD8; Figure 6B). For KTC, single PI3Kα/δ as well as combined inhibitor treatment resulted in complete tumor depletion without visible synergistic effects. For this model, the synergism was only visible when leaving pretreated mice untreated for several days. We observed that AZD8835 pretreated tumors reengrafted significantly faster compared with AZD8835/ibrutinib pretreated tumors ($P = 1.22 \times 10^{-5}$ for AZD8835 vs AZD8835/ibrutinib on day 18; Figure 6B). In summary, these results demonstrate that combined PI3Kα/δ and BTK inhibition seems to be highly effective in ABC DLBCL models in vitro and in vivo.

Discussion

This study identified novel survival addictions to 2 different branches of the PI3K/AKT signaling pathway. AKT signaling is crucial for PTEN-deficient DLBCLs, whereas PI3Kα/δ−induced activation of NF-κB is critical for ABC DLBCLs. Each pathway is activated in an almost exclusive fashion in these subtypes, conferring preferential sensitivity to AKT and PI3Kα/δ inhibitors. Our results were obtained using various in vitro and in vivo models including PDX models that are ideal for drug development due to their strong resemblance to human

Figure 3. AZD5363 regulates MYC signaling in PTEN-deficient DLBCLs. (A) Treatment with 1 μM AZD5363 for 6 and 24 hours results in increased phosphorylation of AKT and decreased PRAS40 phosphorylation in BJAB, K422, and U2932 cells measured by western blotting. (B) Treatment with 1 μM AZD5363 for 6 and 12 hours results in increased phosphorylation of AKT and decreased PRAS40 phosphorylation in UP4FD cells measured by western blotting. (C) GEP following AZD5363 treatment in K422 and U2932 cells. Changes of gene expression are profiled at the indicated time points following treatment with AZD5363. Gene expression changes are depicted according to the color scale shown. Genes that are involved in critical biological processes are highlighted. (D) Gene set enrichment analysis of a previously described MYC gene expression signature. The MYC signature is significantly enriched with genes that are downregulated following AZD5363 treatment in K422 and U2932 cells. (E) AKT inhibition following treatment with 1 μM AZD5363 for 6 and 24 hours results in decreased MYC expression measured by western blotting in BJAB, K422, and U2932 cells. (F) Expression of an *MYC* cDNA partially rescues BJAB and U2932 cells treated with AZD5363. In contrast, expression of an *MYC* cDNA does not rescue cells from doxorubicin-induced toxicity. Expression of exogenous MYC protein is shown by western blotting. Representative results from at least 3 independent replicates are shown. Error bars indicate standard deviations.

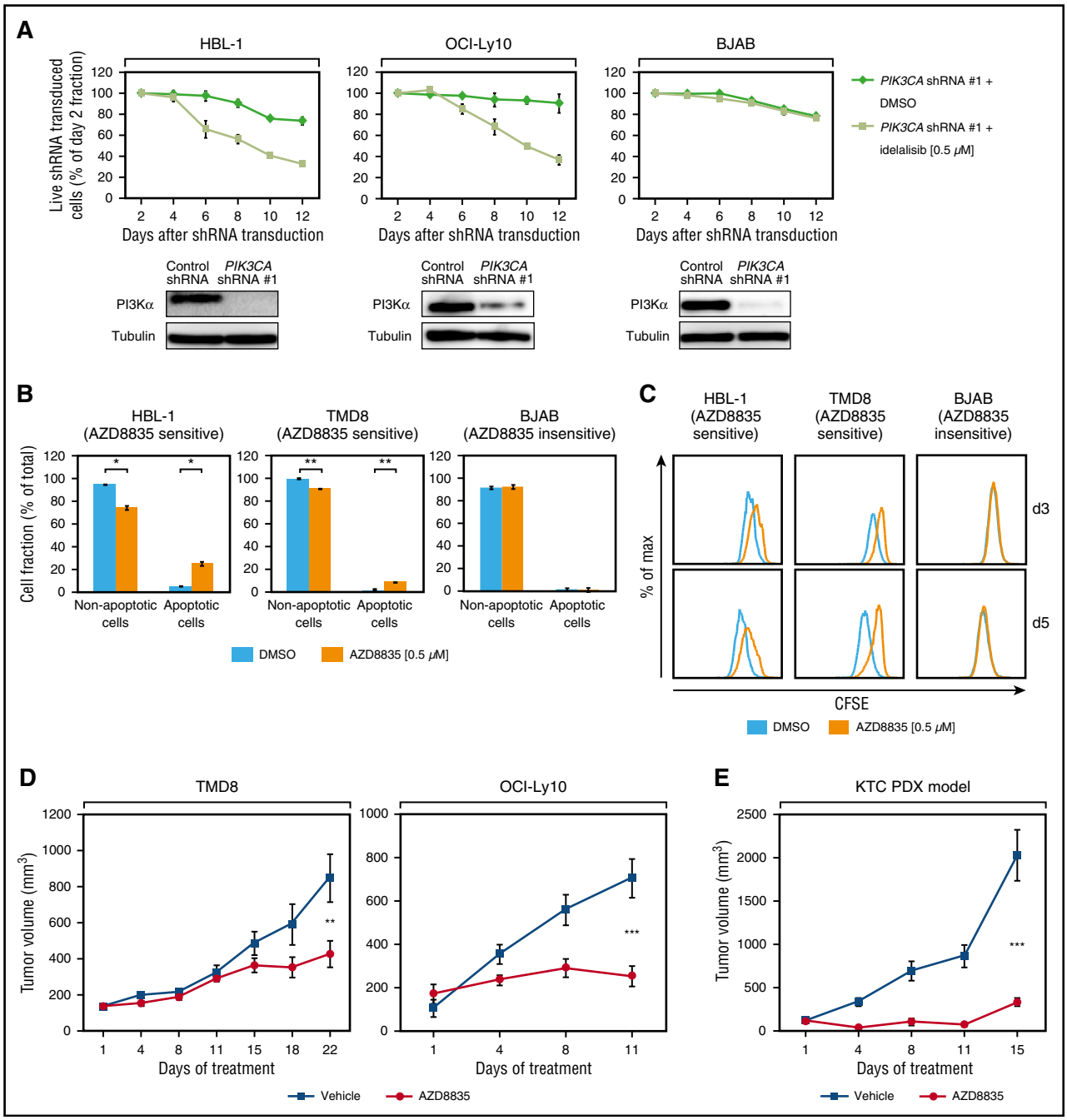

Figure 4. AZD8835 is active in vitro and in vivo in ABC DLBCLs. (A) Downregulation of PI3Kα is required to induce cytotoxicity in HBL-1 and OCI-Ly10 cells treated with the PI3Kδ inhibitor idelalisib. In contrast, BJAB cells that were used as a negative control do not respond to PI3Kα knockdown and idelalisib treatment. Data are expressed as means ± standard deviation of at least 2 independent experiments. (B) PI3Kα/δ inhibition induces apoptosis. AZD8835 increases the rate of apoptotic cells in HBL-1 and TMD8 after 5 days of treatment. Data are expressed as means ± standard deviation of at least 2 independent experiments. (C) AZD8835 treatment reduces cell proliferation. CFSE dilutions after AZD8835 treatment are measured after 3 and 5 days. Cell proliferation is reduced in HBL-1 and TMD8 cells compared with DMSO-treated cells. Representative results of 3 independent experiments are shown. (D) Tumor growth curves of TMD8 and OCI-Ly10 xenograft mouse models following treatment with either AZD8835 (red) or vehicle control (blue). AZD8835 significantly reduces tumor growth in ABC DLBCL xenograft mouse models ($P = .0091$ for AZD8835 [n = 10] vs vehicle [n = 10] on day 22 in TMD8; $P = .0003$ for AZD8835 [n = 9] vs vehicle [n = 9] on day 11 in OCI-Ly10; 1-tailed 2-sample Student *t* tests). Treatment was initiated after animals developed macroscopic signs of tumors (day 6 after engraftment in TMD8; day 24 after engraftment in OCI-Ly10). Error bars indicate the standard error of the mean. (E) Tumor growth curves for KTC PDX mouse model. Treatment with AZD8835 (red) significantly reduces tumor growth compared with the vehicle control (blue) in the KTC mouse model ($P = 5.36 \times 10^{-5}$ for AZD8835 [n = 8] vs vehicle [n = 8] on day 15; 1-tailed 2-sample Student *t* test). Treatment was initiated after animals developed macroscopic signs of tumors (day 15 after engraftment). Error bars indicate the standard error of the mean. *$P < .05$; **$P < .01$; ***$P < .001$.

DLBCL.[36,37] We found that ABC DLBCLs without *CARD11* mutations are addicted to PI3Kα/δ signaling, explaining most likely why the PI3Kδ-specific inhibitor idelalisib did not achieve responses in a small trial conducted in relapsed/refractory DLBCL patients.[15] Our work using a specific shRNA targeting PI3Kα and the PI3Kδ inhibitor idelalisib highlights that resistance to PI3Kδ inhibition can be overcome by simultaneous PI3Kα inhibition. PI3Kα/δ inhibition leads to depletion of NF-κB signaling, indicating a crosstalk

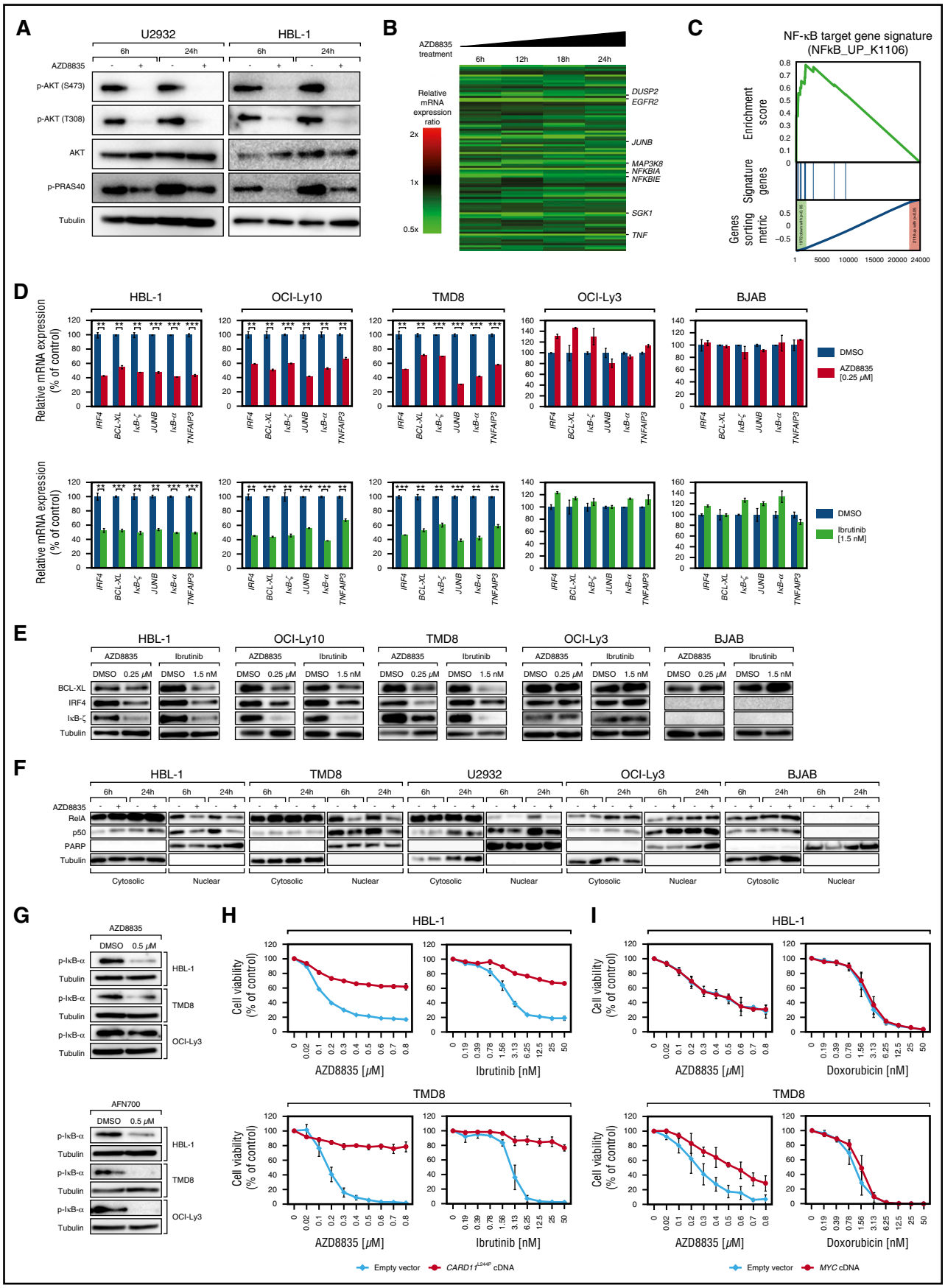

Figure 5.

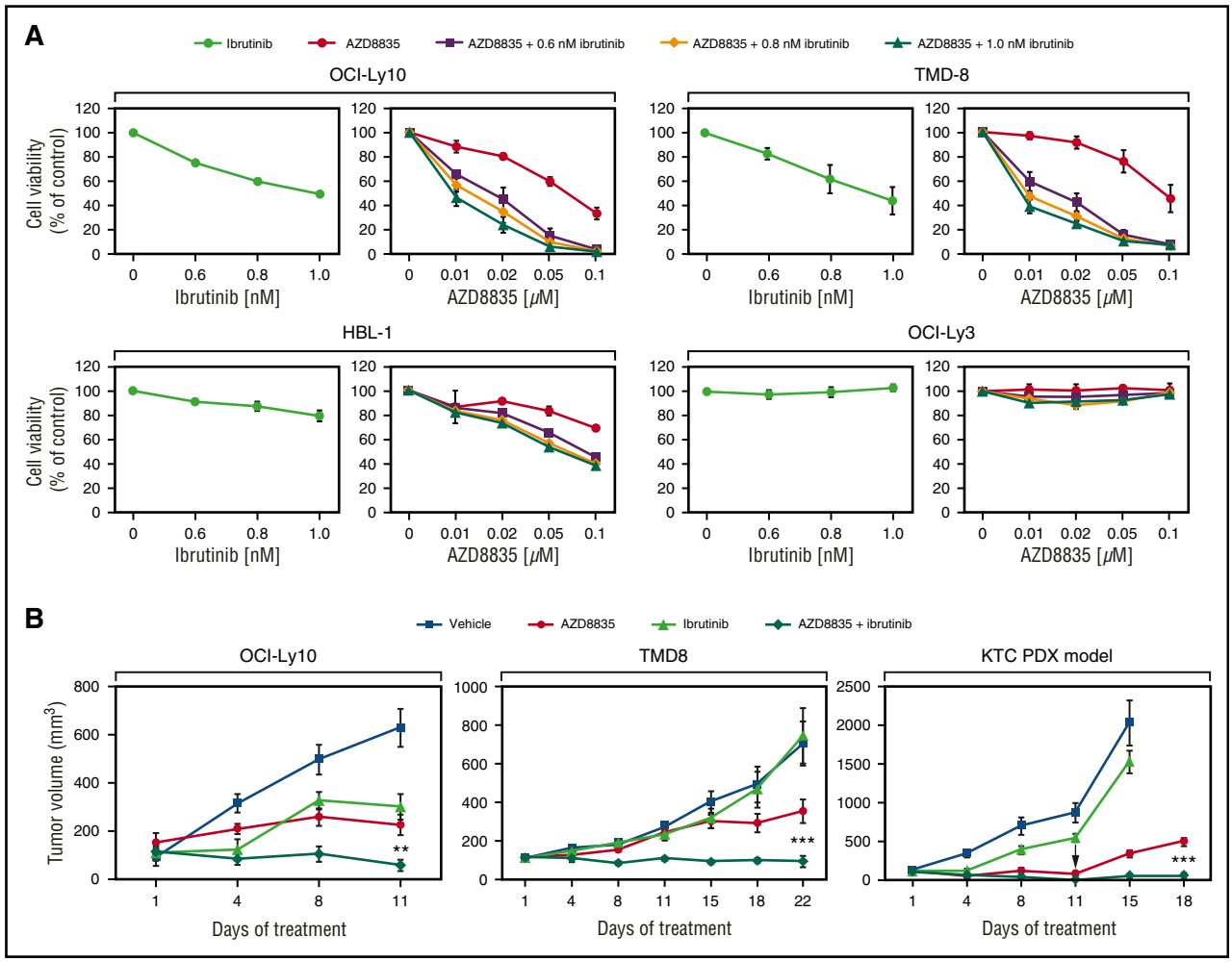

Figure 6. AZD8835 and ibrutinib act synergistically in ABC DLBCLs. (A) AZD8835 and ibrutinib in vitro treatment of OCI-Ly10, TMD8, HBL-1, and OCI-Ly3 cells. Combinatorial treatment induces synergistic cytotoxicity in OCI-Ly10, TMD8, and HBL-1 cells. In contrast, OCI-Ly3 cells are affected by neither single nor combined inhibitor treatment. (B) Tumor growth curves of OCI-Ly10 and TMD8 xenograft mouse models and of the non-GCB DLBCL PDX model KTC following treatment with either vehicle control, AZD8835 alone, ibrutinib alone, or with both AZD8835 and ibrutinib. Combined inhibitor treatment with AZD8835 and ibrutinib reduces tumor growth significantly more compared with AZD8835 alone ($P = .002$ for AZD8835 [n = 9] vs AZD8835/ibrutinib [n = 10] on day 11 in OCI-Ly10; $P = .001$ for AZD8835 [n = 10] vs AZD8835/ibrutinib [n = 10] on day 22 in TMD8; $P = 1.22 \times 10^{-5}$ for AZD8835 [n = 8] vs AZD8835/ibrutinib [n = 8] on day 18 in KTC; 1-tailed 2-sample Student *t* tests). Treatment was initiated after animals developed macroscopic signs of tumors (day 24 after engraftment in OCI-Ly10; day 6 after engraftment in TMD8; day 15 after engraftment in KTC). Error bars indicate the standard error of the mean. The arrow indicates end of treatment with AZD8835 and AZD8835/ibrutinib in the KTC PDX model. $^{**}P < .01$; $^{***}P < .001$.

between both pathways. A possible link between these signaling cascades might represent PDK1 that acts downstream of PI3K as suggested by previous work.[8] Activating *CARD11* mutations seem to cause resistance to PI3Kα/δ inhibition, as *CARD11*-mutated OCI-Ly3 cells were unaffected by PI3Kα/δ inhibition. Likewise, sensitive cells that exogenously express *CARD11* mutations became resistant to AZD8835. In contrast, *MYC* aberrations present in some ABC DLBCLs did not influence sensitivity.

Figure 5. AZD8835 inhibits NF-κB signaling in ABC DLBCLs. (A) Treatment with AZD8835 for 6 and 24 hours decreases both AKT and PRAS40 phosphorylation levels in U2932 and HBL-1 cells measured by western blotting. (B) GEP following treatment with AZD8835 in HBL-1, OCI-Ly10, and U2932 cells. Changes of gene expression are profiled at the indicated time points following treatment with AZD8835. Gene expression changes are depicted according to the color scale shown. Genes that are involved in critical biological processes are highlighted. (C) Gene set enrichment analysis of a previously described NF-κB gene expression signature. The NF-κB signature is significantly enriched with genes that are downregulated after AZD8835 treatment. (D) NF-κB target genes are downregulated on mRNA level in HBL-1, OCI-Ly10, and TMD8 but not in OCI-Ly3 and BJAB cells after treatment with AZD8835. The BTK inhibitor, ibrutinib, that was used as a positive control, downregulates the NF-κB target genes *IRF4*, *BCL-XL*, *IκB-ζ*, *JUNB*, *IκB-α*, and *TNFAIP3* to a similar degree. Representative results from at least 2 independent experiments are shown. Error bars indicate the standard deviation. (E) NF-κB target genes are downregulated on protein levels in HBL-1, OCI-Ly10, and TMD8 cells after treatment with AZD8835 and ibrutinib. No downregulation can be observed in insensitive control cell lines OCI-Ly3 and BJAB. Representative results from at least 3 independent experiments are shown. (F) Analyses of cytosolic and nuclear distribution of NF-κB subunits. Treatment with AZD8835 significantly decreases nuclear expression of the NF-κB subunits RelA and p50 in sensitive HBL-1, TMD8, and U2932 cells, whereas no changes are detectable in insensitive OCI-Ly3 and BJAB models. Successful nuclear and cytosolic fractionation is indicated by tubulin and poly (ADP-ribose) polymerase 1 (PARP) expression. Representative results from 2 independent experiments are shown. (G) AZD8835 treatment inhibits IκB-α phosphorylation in HBL-1 and TMD8 cells. In contrast, p-IκB-α levels are not changed in OCI-Ly3 cells following AZD8835 treatment. The IκB kinase inhibitor AFN700 reduces p-IκB-α levels in all 3 cell lines. Representative results from at least 3 independent experiments are shown. (H) The activating $CARD11^{L244P}$ mutant rescues HBL-1 and TMD8 cells from AZD8835- and ibrutinib-induced cytotoxicity. Data are expressed as means ± standard deviation of at least 2 independent experiments. (I) Exogenous expression of an *MYC* cDNA partially rescues TMD8 cells from AZD8835-induced cytotoxicity, whereas it has no effect on viability of HBL-1 cells. Representative results from at least 3 independent experiments are shown. $^{**}P < .01$; $^{***}P < .001$.

A combined approach of BTK and PI3Kα/δ inhibition using ibrutinib and AZD8835 was highly effective in vitro and in vivo. Ibrutinib as a single agent was tested in a recently completed phase 2 trial.[4] However, this strategy was only moderately active in ABC DLBCLs, as only ~40% of relapsed/refractory ABC DLBCL patients responded.[4] Furthermore, these responses were usually only of short duration. Especially our in vivo PDX model data suggest that combined inhibition of BTK and PI3Kα/δ is substantially more active compared with ibrutinib alone, supporting the results of a previous high-throughput combination screen that showed effectiveness of ibrutinib and PI3K inhibitors in ABC DLBCL models.[38] Collectively, these data provide a therapeutic rationale to combine PI3Kα/δ and BTK inhibitors in future clinical trials.

In contrast to PI3Kα/δ dependency in ABC DLBCLs, PTEN-deficient DLBCLs seem to be addicted to AKT signaling, as the AKT-specific inhibitor AZD5363 induced apoptosis and inhibited cell proliferation predominantly in this DLBCL subgroup. *MYC* aberrations in our models had no impact on inhibitor sensitivity. Interestingly, 2 models with PTEN expression were also sensitive to AZD5363, suggesting that subsets of PTEN-positive DLBCLs might also benefit from AKT inhibition. However, the molecular features determining AKT sensitivity in PTEN-positive DLBCLs are unclear and should be addressed in future work. Sensitivity to AKT inhibition was previously shown in DLBCLs using different AKT inhibitors.[39,40] However, the predominant activity in a molecularly defined subgroup has not yet been described. PTEN deficiency is a hallmark of GCB DLBCLs. Accordingly, the vast majority of sensitive models derive from GCB DLBCL patients.[9] However, 1 of the sensitive cell lines was the PTEN-deficient ABC DLBCL line U2932. This finding suggests a common dependency in ABC and GCB DLBCLs with PTEN loss and argues in favor of a patient selection in clinical trials based on the PTEN expression status rather than on the cell of origin. Inhibition of AKT significantly downregulated expression of MYC, mirroring effects of PTEN reexpression in PTEN-deficient DLBCLs and suggesting that PTEN and AKT target genes overlap at least partially.[9] Interestingly, other previously identified PI3K/AKT signatures were not downregulated following AKT inhibition. This finding is surprising and could be related to the fact that these signatures were created in other settings or disease entities.

In summary, our work highlights that a thorough molecular characterization of DLBCLs is necessary to use novel therapeutic compounds in the most effective manner. Based on our data, PI3Kα/δ inhibitors such as AZD8835 should be tested in clinical studies in ABC DLBCLs without *CARD11* mutations, whereas AKT inhibition using AZD5363 or other specific AKT inhibitors should be investigated in DLBCL patients with PTEN loss.

Acknowledgments

This work was supported by research grants from AstraZeneca, the Deutsche Krebshilfe, the Deutsche Forschungsgemeinschaft (DFG), the Else Kröner-Fresenius-Stiftung, the Brigitte und Dr. Konstanze Wegener-Stiftung, and the Swiss National Science Foundation (Sinergia grant) (G.L.). In addition, this work was supported by the DFG EXC 1003 Cells in Motion-Cluster of Excellence, Münster, Germany (G.L.). Support was provided by the Ministry of Health of the Czech Republic grant AZV 15-27757A and the Grant Agency of the Czech Republic grant GACR14-19590S (P.K.).

Authorship

Contribution: T.E. designed research, performed experiments, analyzed data, and wrote the manuscript; P.K. and J.T.L. performed and analyzed experiments; M. Grau performed bioinformatic and biophysical analyses; P.V., J.M., D.T., K.H., U.M.P., M. Grondine, M.M., B.D., M.P., K.E., and D.S. performed and analyzed experiments; M.Z. performed bioinformatic and biophysical analyses; A.M.S., G.O., W.E.B., B.R.D., F.C., M.T., P.L., and S.T.B. analyzed data; and G.L. designed research, analyzed data, and wrote the manuscript.

Conflict-of-interest disclosure: J.T.L., K.H., U.M.P., M. Grondine, M.M., B.R.D., F.C., and S.T.B. are employees of AstraZeneca. G.L. received research funding from AstraZeneca. The remaining authors declare no competing financial interests.

Correspondence: Georg Lenz, Translational Oncology, University Hospital Münster, Albert-Schweitzer-Campus 1, 48149 Münster, Germany; e-mail: georg.lenz@ukmuenster.de.

References

1. A clinical evaluation of the International Lymphoma Study Group classification of non-Hodgkin's lymphoma. The Non-Hodgkin's Lymphoma Classification Project. *Blood*. 1997; 89(11):3909-3918.
2. Nogai H, Dörken B, Lenz G. Pathogenesis of non-Hodgkin's lymphoma. *J Clin Oncol*. 2011;29(14): 1803-1811.
3. Alizadeh AA, Eisen MB, Davis RE, et al. Distinct types of diffuse large B-cell lymphoma identified by gene expression profiling. *Nature*. 2000; 403(6769):503-511.
4. Wilson WH, Young RM, Schmitz R, et al. Targeting B cell receptor signaling with ibrutinib in diffuse large B cell lymphoma. *Nat Med*. 2015; 21(8):922-926.
5. Gisselbrecht C, Glass B, Mounier N, et al. Salvage regimens with autologous transplantation for relapsed large B-cell lymphoma in the rituximab era. *J Clin Oncol*. 2010;28(27): 4184-4190.
6. Uddin S, Hussain AR, Siraj AK, et al. Role of phosphatidylinositol 3′-kinase/AKT pathway in diffuse large B-cell lymphoma survival. *Blood*. 2006;108(13):4178-4186.
7. Hasselblom S, Hansson U, Olsson M, et al. High immunohistochemical expression of p-AKT predicts inferior survival in patients with diffuse large B-cell lymphoma treated with immunochemotherapy. *Br J Haematol*. 2010; 149(4):560-568.
8. Kloo B, Nagel D, Pfeifer M, et al. Critical role of PI3K signaling for NF-kappaB-dependent survival in a subset of activated B-cell-like diffuse large B-cell lymphoma cells. *Proc Natl Acad Sci USA*. 2011;108(1):272-277.
9. Pfeifer M, Grau M, Lenze D, et al. PTEN loss defines a PI3K/AKT pathway-dependent germinal center subtype of diffuse large B-cell lymphoma. *Proc Natl Acad Sci USA*. 2013;110(30): 12420-12425.
10. Chen L, Monti S, Juszczynski P, et al. SYK inhibition modulates distinct PI3K/AKT-dependent survival pathways and cholesterol biosynthesis in diffuse large B cell lymphomas. *Cancer Cell*. 2013;23(6):826-838.
11. Maehama T, Dixon JE. The tumor suppressor, PTEN/MMAC1, dephosphorylates the lipid second messenger, phosphatidylinositol 3,4,5-trisphosphate. *J Biol Chem*. 1998;273(22): 13375-13378.
12. Cantley LC, Neel BG. New insights into tumor suppression: PTEN suppresses tumor formation by restraining the phosphoinositide 3-kinase/AKT pathway. *Proc Natl Acad Sci USA*. 1999;96(8): 4240-4245.
13. Qing K, Jin Z, Fu W, et al. Synergistic effect of oridonin and a PI3K/mTOR inhibitor on the non-germinal center B cell-like subtype of diffuse large B cell lymphoma. *J Hematol Oncol*. 2016;9(1):72.
14. Zang C, Eucker J, Liu H, et al. Inhibition of pan-class I phosphatidyl-inositol-3-kinase by NVP-BKM120 effectively blocks proliferation and induces cell death in diffuse large B-cell lymphoma. *Leuk Lymphoma*. 2014;55(2): 425-434.
15. Kahl BS, Byrd JC, Flinn IW. Clinical safety and activity in a phase 1 study of CAL-101, an isoform-selective inhibitor of phosphatidylinositol 3-kinase

P110δ, in patients with relapsed or refractory non-Hodgkin lymphoma [abstract]. *Blood*. 2010; 116(21). Abstract 1777.

16. Ngo VN, Davis RE, Lamy L, et al. A loss-of-function RNA interference screen for molecular targets in cancer. *Nature*. 2006;441(7089): 106-110.
17. Nogai H, Wenzel SS, Hailfinger S, et al. IκB-ζ controls the constitutive NF-κB target gene network and survival of ABC DLBCL. *Blood*. 2013; 122(13):2242-2250.
18. Dai B, Grau M, Juilland M, et al. B-cell receptor-driven MALT1 activity regulates MYC signaling in mantle cell lymphoma. *Blood*. 2017;129(3): 333-346.
19. Pfeifer M, Zheng B, Erdmann T, et al. Anti-CD22 and anti-CD79B antibody drug conjugates are active in different molecular diffuse large B-cell lymphoma subtypes. *Leukemia*. 2015;29(7): 1578-1586.
20. Wenzel SS, Grau M, Mavis C, et al. MCL1 is deregulated in subgroups of diffuse large B-cell lymphoma. *Leukemia*. 2013;27(6):1381-1390.
21. Barlaam B, Cosulich S, Delouvrié B, et al. Discovery of 1-(4-(5-(5-amino-6-(5-tert-butyl-1,3,4-oxadiazol-2-yl)pyrazin-2-yl)-1-ethyl-1,2,4-triazol-3-yl)piperidin-1-yl)-3-hydroxypropan-1-one (AZD8835): a potent and selective inhibitor of PI3Kα and PI3Kδ for the treatment of cancers. *Bioorg Med Chem Lett*. 2015;25(22):5155-5162.
22. Davies BR, Greenwood H, Dudley P, et al. Preclinical pharmacology of AZD5363, an inhibitor of AKT: pharmacodynamics, antitumor activity, and correlation of monotherapy activity with genetic background. *Mol Cancer Ther*. 2012; 11(4):873-887.
23. Hudson K, Hancox UJ, Trigwell C, et al. Intermittent high-dose scheduling of AZD8835, a novel selective inhibitor of PI3Kα and PI3Kδ, demonstrates treatment strategies for PIK3CA-dependent breast cancers. *Mol Cancer Ther*. 2016;15(5):877-889.
24. Weilemann A, Grau M, Erdmann T, et al. Essential role of IRF4 and MYC signaling for survival of anaplastic large cell lymphoma. *Blood*. 2015;125(1):124-132.
25. Davis RE, Ngo VN, Lenz G, et al. Chronic active B-cell-receptor signalling in diffuse large B-cell lymphoma. *Nature*. 2010;463(7277):88-92.
26. Klanova M, Andera L, Brazina J, et al. Targeting of BCL2 family proteins with ABT-199 and homoharringtonine reveals BCL2- and MCL1-dependent subgroups of diffuse large B-cell lymphoma. *Clin Cancer Res*. 2016;22(5): 1138-1149.
27. Okuzumi T, Fiedler D, Zhang C, et al. Inhibitor hijacking of Akt activation. *Nat Chem Biol*. 2009; 5(7):484-493.
28. Culhane AC, Schröder MS, Sultana R, et al. GeneSigDB: a manually curated database and resource for analysis of gene expression signatures. *Nucleic Acids Res*. 2012;40(Database issue):D1060-D1066.
29. Gray KA, Daugherty LC, Gordon SM, Seal RL, Wright MW, Bruford EA. Genenames.org: the HGNC resources in 2013. *Nucleic Acids Res*. 2013;41(Database issue):D545-D552.
30. Liberzon A, Subramanian A, Pinchback R, Thorvaldsdóttir H, Tamayo P, Mesirov JP. Molecular signatures database (MSigDB) 3.0. *Bioinformatics*. 2011;27(12):1739-1740.
31. Shaffer AL, Wright G, Yang L, et al. A library of gene expression signatures to illuminate normal and pathological lymphoid biology. *Immunol Rev*. 2006;210:67-85.
32. Subramanian A, Tamayo P, Mootha VK, et al. Gene set enrichment analysis: a knowledge-based approach for interpreting genome-wide expression profiles. *Proc Natl Acad Sci USA*. 2005;102(43):15545-15550.
33. Naylor TL, Tang H, Ratsch BA, et al. Protein kinase C inhibitor sotrastaurin selectively inhibits the growth of CD79 mutant diffuse large B-cell lymphomas. *Cancer Res*. 2011;71(7):2643-2653.
34. Lenz G, Davis RE, Ngo VN, et al. Oncogenic CARD11 mutations in human diffuse large B cell lymphoma. *Science*. 2008;319(5870):1676-1679.
35. Ceribelli M, Kelly PN, Shaffer AL, et al. Blockade of oncogenic IκB kinase activity in diffuse large B-cell lymphoma by bromodomain and extraterminal domain protein inhibitors. *Proc Natl Acad Sci USA*. 2014;111(31):11365-11370.
36. Townsend EC, Murakami MA, Christodoulou A, et al. The public repository of xenografts enables discovery and randomized phase II-like trials in mice. *Cancer Cell*. 2016;29(4):574-586.
37. Chapuy B, Cheng H, Watahiki A, et al. Diffuse large B-cell lymphoma patient-derived xenograft models capture the molecular and biological heterogeneity of the disease. *Blood*. 2016; 127(18):2203-2213.
38. Mathews Griner LA, Guha R, Shinn P, et al. High-throughput combinatorial screening identifies drugs that cooperate with ibrutinib to kill activated B-cell-like diffuse large B-cell lymphoma cells. *Proc Natl Acad Sci USA*. 2014;111(6):2349-2354.
39. Petrich AM, Leshchenko V, Kuo PY, et al. Akt inhibitors MK-2206 and nelfinavir overcome mTOR inhibitor resistance in diffuse large B-cell lymphoma. *Clin Cancer Res*. 2012;18(9): 2534-2544.
40. Ezell SA, Wang S, Bihani T, et al. Differential regulation of mTOR signaling determines sensitivity to AKT inhibition in diffuse large B cell lymphoma. *Oncotarget*. 2016;7(8):9163-9174.
41. Trabucco SE, Gerstein RM, Evens AM, et al. Inhibition of bromodomain proteins for the treatment of human diffuse large B-cell lymphoma. *Clin Cancer Res*. 2015;21(1):113-122.
42. Mehra S, Messner H, Minden M, Chaganti RS. Molecular cytogenetic characterization of non-Hodgkin lymphoma cell lines. *Genes Chromosomes Cancer*. 2002;33(3):225-234.
43. Chang H, Blondal JA, Benchimol S, Minden MD, Messner HA. p53 mutations, c-myc and bcl-2 rearrangements in human non-Hodgkin's lymphoma cell lines. *Leuk Lymphoma*. 1995; 19(1-2):165-171.
44. Farrugia MM, Duan LJ, Reis MD, Ngan BY, Berinstein NL. Alterations of the p53 tumor suppressor gene in diffuse large cell lymphomas with translocations of the c-MYC and BCL-2 proto-oncogenes. *Blood*. 1994;83(1):191-198.
45. Al-Katib AM, Smith MR, Kamanda WS, et al. Bryostatin 1 down-regulates mdr1 and potentiates vincristine cytotoxicity in diffuse large cell lymphoma xenografts. *Clin Cancer Res*. 1998; 4(5):1305-1314.